Journal of Pharmaceutical and Biomedical Analysis 55 (2011) 342–348

Contents lists available at ScienceDirect

Journal of Pharmaceutical and Biomedical Analysis

journal homepage: www.elsevier.com/locate/jpba

Evaluation of pharmacokinetic and pharmacodynamic relationship for oral sustained-release atenolol pellets in rats

Junting Jia, Chendong Dong, Wenli Zhang, Yanxia Cui, Jianping Liu *

Department of Pharmaceutics, China Pharmaceutical University, Nanjing, PR China

ARTICLE INFO

Article history:
Received 20 September 2010
Received in revised form 14 January 2011
Accepted 22 January 2011

Keywords:
Atenolol
Pharmacokinetics
Pharmacodynamics
Sustained-release pellets
PK–PD relationship

ABSTRACT

This study was designed to evaluate the *in vitro* release, pharmacokinetics (PK), pharmacodynamics (PD) and PK–PD relationships of atenolol sustained-release pellets (AT-SRPs), compared with those of atenolol immediate-release pellets (AT-IRPs). Blood sampling for AT plasma concentration was performed in normal rats and blood pressure-lowering effects were recorded continuously in hypertensive rats (HRs) before and at 1, 4, 8, 12, 16 and 24 h after drug administration. The parameters were calculated using DAS1.0 program and WinNonlin software. The release profile of SRPs was steadier and more sustained than that of IRPs. The mean C_{max} and area under concentration–time curve from 0 to 24 h after administration ($AUC_{0-24\,h}$) of SRPs were significantly lower than that of IRPs ($p < 0.05$), while area under concentration–time curve from 0 to infinity ($AUC_{0-\infty}$) was almost equivalent between the two formulations. The mean half life time ($t_{1/2}$) of AT-SRPs was almost 2 times longer compared to that of AT-IRPs. The SRPs approximately achieved half of peak drug effect (E_{max}) of IRPs, while there were no significant differences in the area under effect–time curve from 0 to 24 h after administration ($AUEC_{0-24\,h}$) and the area under effect–time curve from 0 to infinity ($AUEC_{0-\infty}$). The value of the rate constant of equilibration between plasma and the effect-site (k_{e0}) for SRPs was about 4 times higher than IRPs. The effect–concentration–time course for AT-SRPs was represented by the clockwise hysteresis loop, while the counter-clockwise hysteresis loop well showed that for AT-IRPs. The more favorable characteristics of SRPs would make it more appropriate as a potential dosage form for the treatment of hypertension.

1. Introduction

β-Blockers have long been prescribed widely in diverse cardiovascular diseases, *e.g.*, hypertension, angina pectoris, arrhythmias, and myocardial infarction. Moreover, AT is a β-blocker widely used alone or in combination to treat hypertension. Administration of conventional AT tablets has been reported to exhibit fluctuations in plasma drug levels, resulting in either side effects like hypopiesia, bradycardia, dizziness, gastrointestinal (GI) upset and acra-algidity or reduction in the concentration at the receptor site [1,2]. Further, the current therapy is suboptimal as it is commonly administered at high doses (as oral tablets, 100 mg/day) to achieve effective hypotension treatment. AT is incompletely absorbed from the GI tract of human with an absorption ranging from 28% to 47%, and a bioavailability of just 36% of the whole dose [3]. The high polarity dictates its fast renal elimination with no significant metabolism. Moreover, the hypotensive effect of cardiovascular drugs would have been brought into full play, only if the blood pressure was reduced steadily [4]. Therefore, many efforts have been made to improve its pharmaceutical formulation in order to optimize the therapy.

These efforts have been focused on the development of oral sustained-release (SR) preparations, which could increase time available for drug absorption, leading to an increase in drug bioavailability, and a decrease in fluctuation of plasma drug concentration which reduces the side effects. Accordingly, studies have been reported on regulation of AT release using diverse controlled release systems such as osmotic pumps [1,2,5,6], mucoadhesive microspheres [7], mucoadhesive tablets [8], transdermal delivery systems [9,10], and floating controlled delivery systems [11,12]. Composed of multiple units, SRPs have been formulated as the desired preparations for its remarkable advantages, such as homogeneous distribution in GI tract thus maximizing drug absorption, reducing the risk of local GI tract irritation, decreasing dosing frequency, increasing patient compliance and improving the safety and efficacy [13]. Therefore, in this study, AT-SRPs were developed for the treatment of hypertension with a single daily dose.

The PK principles of AT are generally well understood and taken into consideration in the development of drug delivery system

Abbreviations: AT, atenolol; SRPs, sustained-release pellets; IRPs, immediate-release pellets; PK, pharmacokinetics; PD, pharmacodynamics; HRs, hypertensive rats; SBP, systolic pressure.

* Corresponding author. Tel.: +86 25 83271293; fax: +86 25 83271293.
E-mail address: liujianpingljp@hotmail.com (J. Liu).

0731-7085/$ – see front matter © 2011 Elsevier B.V. All rights reserved.
doi:10.1016/j.jpba.2011.01.044

[14,15], while the PD aspects are less studied. In many cases, the main objective of developing SR dosage forms is to reduce the dosing frequency or fluctuation of plasma drug concentrations [16]. The development process of dosage forms tends to be based on an assumption that the magnitude of response elicited by the drug is completely synchronous with the changes in its plasma concentration [17,18]. However, not all changes of drug effects are completely identical with that of plasma concentrations. Thus, it is necessary to evaluate the relationship between the PK and PD. PK–PD modeling, the mathematical description of the relationship between PK and PD, can estimate and predict relevant parameters associated with onset, magnitude and time courses of dose–concentration–effect of a drug [19]. An appropriate PK–PD model is particularly important to judge the ascription of effect site, and optimize various drug delivery systems [20,21].

In previous work [22], we have optimized the formulations of AT-SRPs by evaluating drug release characteristics. In the present study, we have investigated the *in vitro* release behavior and *in vivo* PK and PD characteristics of AT-IRPs and AT-SRPs; meanwhile, PK–PD relationships for the two formulations were analyzed.

2. Materials and methods

2.1. Materials

AT was purchased from Jianyuan Chemical Co., Ltd. (Hubei, China). Metronidazole (MTZ) was purchased from National Institutes for Food and Drug Control (Beijing, China). HPMC-E5, HPMC-E3 and ethylcellulose aqueous dispersion (Surelease® E-7-19040) were gifts from Colorcon (USA). PVPK 29/32 and MCC PH101 were kindly provided by ISP and FMC (USA), respectively. PEG-6000 was purchased from Xilong Chemical Plant (Shantou, China). All other chemicals were of analytical or HPLC grade and purchased from Chemical Reagent Co., Ltd. (Nanjing, China).

2.2. Animals

Adult male Sprague–Dawley rats (weight, 200 ± 20 g) were purchased from Experimental Animal Center of China Pharmaceutical University. The animals were housed under standard conditions with a 12 h light/dark cycle with free access to water and a basal diet for 1 week.

2.3. Preparation of pellets

AT-loaded IR pellets were prepared by extrusion–spheronization method, in which AT, MCC, hexanedioic acid, PVPP were mixed at the weight ratio of 25:64:10:1. After blending the dry excipients sufficiently, the binder solution (3% PVP-K30) was poured and mixed until wet mass was obtained. The wet mass was extruded and spheronized in an extrusion–spheronization apparatus (JBZ-300 multifunctional pelleting and coating machine, YILIAN new-drug research institute, China). The resulting pellets were dried in hot air oven at 40 °C for 12 h, and then screened through 20–32 meshes. The SRPs were prepared in a Mini-Glatt fluidizing bed (Glatt Company, German) by coating the above-mentioned IRPs with aqueous dispersion containing HPMC-E5 as a pore-forming agent and Surelease®. The IR and SR formulations were separately filled into the 5 size hard gelatin capsules.

2.4. In vitro dissolution tests

Dissolution of AT from the pellets was measured using a capacity medicament dissolution and infiltration apparatus (Tianjin University) (ChP, method I). The release profiles of AT from pellets containing 4 mg of drug were determined in 900 mL of pH 6.8 phosphate buffer at a rotating speed of 100 ± 0.5 rpm and 37 ± 0.5 °C. Three milliliter samples were withdrawn and replaced with an equal volume of dissolution medium using a sampler at 1, 2, 4, 8, 12 and 24 h. The sample solution was diluted and measured in a spectrophotometer at a wavelength of 274 nm. The mean values of six determinations were used to calculate the drug release from each formulation.

2.5. Pharmacokinetic studies

2.5.1. Plasma sample preparations

Ten Sprague–Dawley rats were fasted with water access for 12 h prior to initiation of the study and randomly divided into two groups. Then, the rats were orally administered AT-SRPs or AT-IRPs at the same dose of 16 mg/kg. Rats were anesthetized by ether, and blood (0.5 mL) was taken from retro-orbit sinus through heparinized capillary tubes just before and at 1, 4, 8, 12, 16 and 24 h after dosing. Plasma specimens were separated by centrifugation at 1000 rpm for 2 min and stored at −20 °C until analysis.

2.5.2. Sample extraction and analytical procedures

Extraction of AT was set out using a modified version of an earlier reported procedure [23]. Prior to the extraction, frozen plasma samples were thawed at ambient temperature. Rats plasma (100 μL) was mixed with 10 μL of internal standard solution (MTZ, 54 μg mL^{-1}). Then sodium hydroxide solution (1 mol L^{-1}, 150 μL), used to alkalify the sample, was thoroughly added and mixed by vortexing vigorously for 3 min at ambient temperature. Dichloromethane (2 mL) was then added to the mixture and vortex-mixed again for 5 min to extract AT. The samples were centrifuged at 4000 rpm for 8 min. After that, the organic layer was collected and evaporated to dryness under nitrogen flow at 42 °C. The resulting pellet was resuspended in 100 μL of methanol, vortex-mixed for 1 min and 20 μL of the extracted plasma was injected into the HPLC system for analysis.

Plasma AT concentrations were determined by high pressure liquid chromatography (HPLC, Shimadzu LC-10A, Kyoto, Japan) equipped with an ultraviolet (UV) detection, a Shim-pack VP-ODS (150 mm × 4.6 mm) column. The detection wavelength was 274 nm. The mobile phase consisted of acetonitrile, distilled water and triethylamine (5:95:0.02, v/v/v). The flow rate was 0.7 mL min^{-1}, and the column temperature was set at 40 °C.

2.5.3. Calibration curve

The AT stock solution (100 μg mL^{-1}) was prepared in methanol and stored at 4 °C. Then working solutions were prepared by diluting the stock solution in methanol. 100 μL of these serial dilutions were transferred into 1.5 mL Eppendorf tubes and the solvents were evaporated to dryness under nitrogen. The resulted samples were then used to spike the blank rat plasma (100 μL) and the following procedures were done as described in Section 2.5.2. A calibration curve at 0.02, 0.05, 0.1, 0.2, 0.5, 1.0 and 2.0 μg mL^{-1} AT in rat plasma was generated.

2.5.4. Method validation

Method validation including recovery, specificity, within- and between-day precision of HPLC was carried out.

2.6. Pharmacodynamics

To produce hypertension, rats were fed with high-fat and high-sucrose diets for 40 days freely. The blood pressure was measured after that using the tail-cuff method, and rats with the systolic pressure (SBP) > 130 mm Hg were then selected for the experiment. The HRs (n = 15) were randomly divided into three groups: (1)

controlled group, received a controlled capsule containing blank pellets without AT ($n = 5$); (2) IR group, received a capsule containing AT-IRPs (dose 16 mg/kg, $n = 5$); (3) SR group, received a capsule containing AT-SRPs (dose 16 mg/kg, $n = 5$). SBP levels were measured just before and at 1, 4, 8, 12, 16, and 24 h after administration.

For the SR and IR groups, blood pressure-lowering effect at time t was calculated according to the formula:

$$(\Delta SBP)_t = (SBP_{control})_t - SBP_t \quad (1)$$

where ΔSBP is the change of SBP, $SBP_{control}$ is SBP value of the control group, SBP_t is SBP value of AT-SRPs or AT-IRPs at time t.

2.7. Data analysis

Analysis of PK and PD data was performed. In the first stage, the PK curve-fittings were done for two data sets: mean plasma concentration and time data. In the second stage, the PK–PD models were fitted to the mean ΔSBP and time profiles using the estimated PK parameters as fixed values.

2.8. PK parameter estimation and statistical analysis

The pharmacokinetic analysis of the AT concentration–time data in rats were performed using DAS program (version1.0, Pharmacometrics Professional Committee of China, Shanghai, China) and the compartmental pharmacokinetic parameters were calculated. Both one- and two-compartment models were characterized and the most appropriate pharmacokinetic models were determined using the Akaike information criterion (AIC). The pharmacokinetics of AT from IRPs and SRPs were fitted to one-compartment models. The PK estimation was characterized by the following parameters: AUC, C_{max}, t_{max}, $t_{1/2}$, k_{10} (the elimination rate constant), and k_a (the absorption rate constant).

2.9. PK–PD relationship

The maximum antihypertensive action (ΔSBP_{max}) was determined from ΔSBP–time profile, and AUEC was calculated by the trapezoidal rule. Analysis of PD data was performed using the WinNonlin program (Version 5.2.1, Pharsight Corporation, USA), which was accomplished in the test period. The PK–PD model with a separated effect compartment was adopted for the analysis of the data. The effect-site drug concentration (C_e) and central compartment drug concentration (C) are expressed as Eqs. (2) and (3), respectively [24]:

$$C_e = \frac{X_0 \cdot k_a \cdot k_{e0}}{V'} \cdot \left[\frac{e^{-k_a t}}{(k_{10} - k_a)(k_{e0} - k_a)} + \frac{e^{-k_{10} t}}{(k_a - k_{10})(k_{e0} - k_{10})} + \frac{e^{-k_{e0} t}}{(k_a - k_{e0})(k_{10} - k_{e0})} \right] \quad (2)$$

$$C = \frac{F X_0 k_a}{V_d (k_a - k_{10})} \cdot (e^{-k_{10} t} - e^{-k_a t}) = \frac{X_0 k_a}{V' (k_a - k_{10})} \cdot (e^{-k_{10} t} - e^{-k_a t}) \quad (3)$$

where X_0 is the dose, V_d is the volume of distribution, F is the oral bioavailability, V' is the quotient of V_d/F, k_{e0}, other parameters are identical to those previously mentioned.

A non-linear regression of C_e and ΔSBP data was carried out using the computer program WinNonlin by means of following formula:

$$\Delta SBP = \frac{E_{max} \times C_e}{C_e + EC_{50}} \quad (4)$$

where ΔSBP is the change of SBP; EC_{e50} is the AT concentration in the effect compartment yielding half maximal effect.

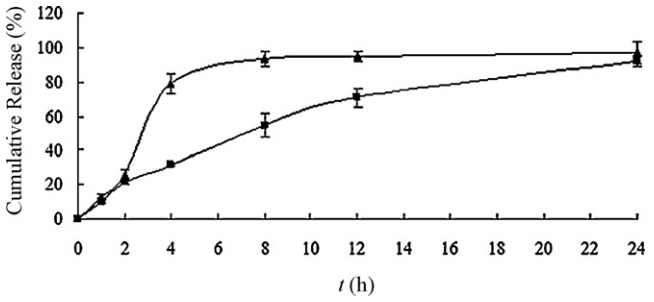

Fig. 1. The release profiles of AT from IR or SR formulation (mean ± SD, $n = 6$): (▲) IRPs and (■) SRPs.

Table 1
Absolute recovery of AT from spiked rat plasma ($n = 5$).

Nominal concentration (μg mL^{-1})	Recovery (%)	SD (%)
0.05	81.34	4.23
0.5	84.24	3.78
2	83.56	2.89

2.10. Statistical analysis

Data were expressed as mean ± SD of five animals. Statistical analysis was performed using t-test. Statistical significance was defined as $p < 0.05$.

3. Results

3.1. In vitro release

Fig. 1 illustrates the release profiles of the two formulations. The release behaviors of both formulations were similar at the first 2 h, while great difference was observed after 2.5 h. The release rate of AT from SRPs was much slower than that from IRPs, 90% of AT was released after 24 h from the former but after 5 h from the latter (Fig. 1).

3.2. Pharmacokinetics

3.2.1. Method validations

3.2.1.1. Specificity. Under the elution conditions, AT and MTZ were well separated from the matrix impurities, with retention times at 14.07 and 17.23 min, respectively (Fig. 2).

3.2.1.2. Recovery. The absolute recovery of AT and MTZ was determined by comparing the amount measured in blank plasma samples spiked with standard solutions, relative to standard solutions at the same concentration. As it can be seen from Table 1, the absolute recovery of spiked AT ranged from 81% to 84% at three concentrations tested.

3.2.1.3. Range and linearity of the calibration curve. A calibration curve was constructed for AT at the concentrations indicated above. The linear range was 0.02–2.0 μg mL^{-1}, and the equation of calibration curve was $y = 0.2783x + 0.0052$, with $R^2 = 0.9936$.

3.2.1.4. Within- and between-day precision. Blank rat plasma samples were spiked in five replicates with AT at 0.05, 0.5, 5 μg mL^{-1} and immediately processed at ambient temperature. The within day precision was displayed as the relative standard deviation (RSD) from 5 repeats in a single run. The between-day precision was RSD from the mean measurements among 3 different runs.

The results of within- and between-day precision were shown in Table 2 and the RSDs were within the acceptable range of 10%.

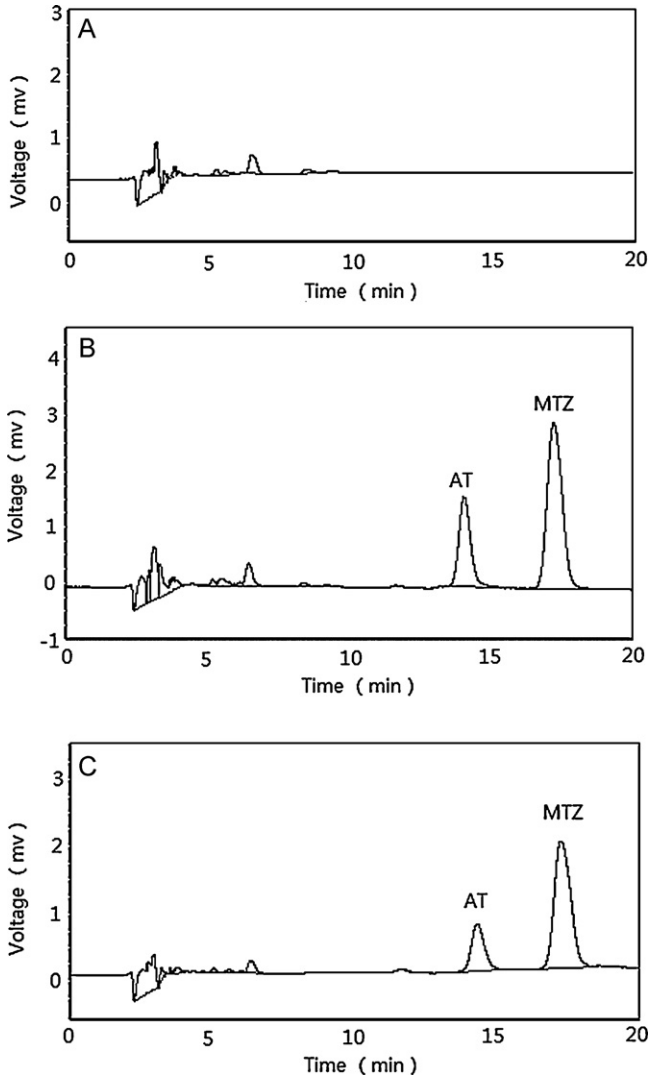

Fig. 2. Representative chromatograms: (A) blank rat plasma sample; (B) rat plasma sample spiked with AT at 0.5 μg/mL; (C) rat plasma sample after oral administration of AT pellets.

Table 2
Measurement precision for AT in spiked rat plasma.

Nominal concentration ($\mu g\,mL^{-1}$)	Measured concentration ($\mu g\,mL^{-1}$)	[a]WDP (%)	[b]BDP (%)
0.05	0.0509	4.87	4.32
0.5	0.506	2.77	4.14
2	2.03	1.95	2.46

[a] WDP (%), within day precision.
[b] BDP (%), between day precision.

3.2.2. PK analysis

Fig. 3 displays mean plasma AT concentration *versus* time profiles after single-dose administration of the IR and SR formulations in normal rats and the estimated PK parameters were listed in Table 3.

As shown in Fig. 3, C_{max} of AT-SRPs was much lower than that of AT-IRPs, while trough plasma concentration (C_{min}) was almost identical between them, indicating that the fluctuation between C_{max} and C_{min} was greatly reduced in SR group.

The values in t_{max} for IRPs and SRPs were 2.7 h and 9.78 h, respectively, but after t_{max}, the plasma concentration declined in the latter more gradually than the former. The $AUC_{0-24\,h}$ value of SRPs was

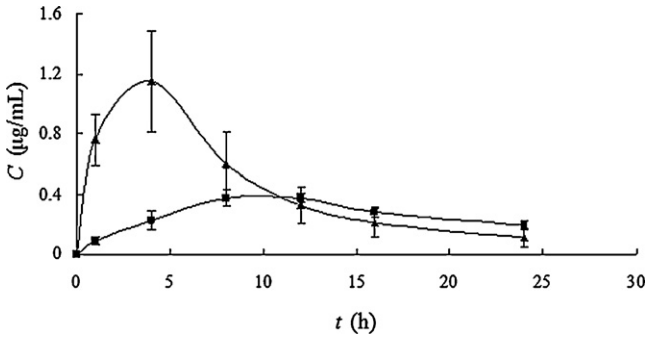

Fig. 3. Plots of plasma AT concentrations *versus* time after single oral administration of IR and SR formulation to normal rats (mean ± SD, $n = 5$, 16 mg/kg): (▲) IRPs and (■) SRPs.

Table 3
Pharmacokinetic parameters for AT from IR and SR formulations after single oral administration to normal rats.

Parameters (unit)	Value	
	AT-IRPs	AT-SRPs
k_a (h^{-1})	0.704 ± 0.337	0.107 ± 0.009[a]
k_{10} (h^{-1})	0.194 ± 0.077	0.099 ± 0.011[a]
$t_{1/2}$ (h)	4.059 ± 1.550	7.080 ± 0.833[a]
C_{max} ($\mu g\,mL^{-1}$)	1.165 ± 0.214	0.355 ± 0.036[a]
t_{max} (h)	2.777 ± 0.712	9.780 ± 0.968[a]
$AUC_{0-24\,h}$ ($h\,\mu g\,mL^{-1}$)	10.928 ± 2.784	6.600 ± 0.539[a]
$AUC_{0-\infty}$ ($h\,\mu g\,mL^{-1}$)	11.281 ± 2.806	9.388 ± 0.553

Data are means ± SD of five rats.
[a] $P < 0.05$ *versus* AT-IRPs.

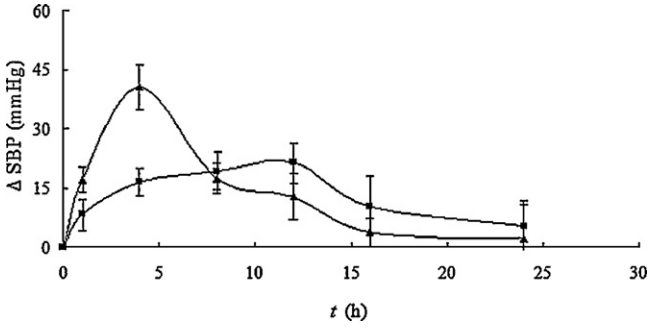

Fig. 4. Plots of ΔSBP *versus* time after a single oral administration of IR and SR formulation to HRs (mean ± SD, $n = 5$, 16 mg/kg): (▲) IRPs and (■) SRPs.

significantly lower than that of IRPs ($p < 0.05$). However, no significant difference ($p > 0.05$) in $AUC_{0-\infty}$ values was found between the two groups. In another hand, $t_{1/2}$ of SR formulation was significantly extended (Table 3). Otherwise, the individual variances in C_{max}, $AUC_{0-24\,h}$ and $AUC_{0-\infty}$ were smaller for SRPs than for IRPs.

3.3. PK–PD relationship

Fig. 4 shows the temporal profiles of ΔSBP in HRs. In the IR group, the $(\Delta SBP)_{max}$ was 40.6 mm Hg at 4 h, and then the hypotensive effect reduced quickly; while in the SR group, the $(\Delta SBP)_{max}$ was 21.5 mm Hg at 12 h, then the effect decreased gradually.

Meanwhile, the correlation between hypotensive effect and time was simulated for both formulations, and the PK–PD parameters (E_{max}, EC_{50}, k_{e0}, $t_{1/2eq}$, $AUEC_{0-24\,h}$, and $AUEC_{0-\infty}$) were calculated (Table 4). Significant differences were found in all parameters except for $AUEC_{0-24\,h}$ and $AUEC_{0-\infty}$ between IR and SR formulations. Compared with IR group, E_{max}, EC_{50},

Table 4
PK/PD parameters of AT from IR and SR formulations after single oral administration to HRs.

Parameters (unit)	Values	
	AT-IRPs	AT-SRPs
E_{max} (mm Hg)	40.56 ± 0.29	21.52 ± 1.34[a]
EC_{50} (μg mL^{-1})	0.550 ± 0.013	0.173 ± 0.011[a]
k_{e0} (h^{-1})	2.46 ± 0.43	9.99 ± 0.79[a]
$t_{1/2eq}$ (h)	0.28 ± 0.04	0.07 ± 0.003[a]
$AUEC_{0-24\,h}$ (h mm Hg)	330.6 ± 25.372	324.59 ± 13.629
$AUEC_{0-\infty}$ (h mm Hg)	330.933 ± 10.423	338.935 ± 34.437

Data are means ± SD of five rats.
[a] $P < 0.05$ *versus* AT-IRPs.

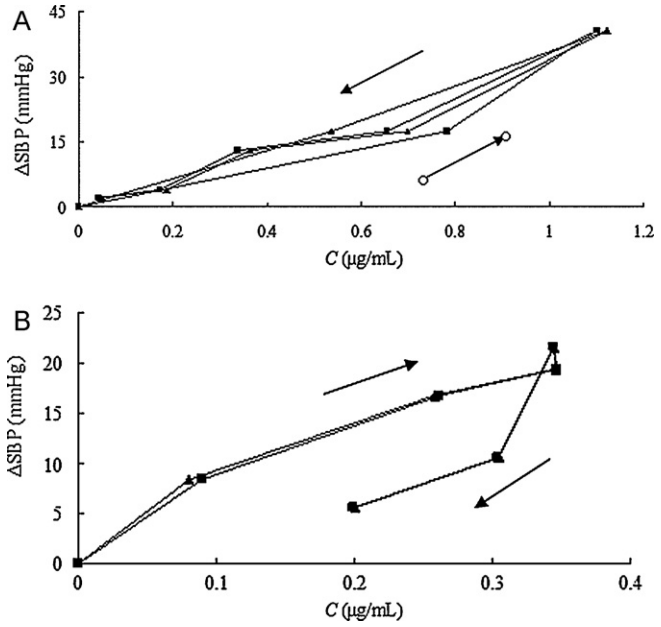

Fig. 5. Temporal Plots of ΔSBP *versus* AT concentration after single oral administration of IR and SR formulation to HRs ($n = 5$, 16 mg/kg). (A) IRPs and (B) SRPs. The arrow indicates the time flow after oral administration. (■) AT concentration in the central compartment and (▲) AT concentration in the effect compartment.

and $t_{1/2eq}$ for SR were notably lower, and k_{e0} was remarkably greater.

3.4. Effect–concentration–time curves

To identify the differences in effect–concentration–time (ECT) curves of AT from the produced formulations, hysteresis loops were plotted based upon the concentration data of central or effect compartments and hypotensive effect at different time points.

As shown in Fig. 5A, a counter-clockwise hysteresis loop was presented between plasma or effect site AT concentration and the hypotensive effect following IRPs administration. In these loops, the effect increased with time for a given drug concentration. The ECT curve for effect compartment was leftward to that for central compartment.

In Fig. 5B, a clockwise hysteresis loop was depicted between plasma or effect site AT concentration and the hypotensive effect following SRPs administration. In the two loops, the drug effect decreased with time at the same concentration. The loop for blood compartment was almost overlapped with that for effect compartment.

It was also characterized that the fast and short-lasting pressure-lowering effect of AT was well represented by a counter-clockwise hysteresis mode for IRPs, while the long-lasting pressure-lowering effect of AT was well reflected by clockwise hysteresis mode for SRPs (Fig. 5A and B).

4. Discussion

In present study, the author estimated the release behavior of AT *in vitro*, PK, PD and PK–PD relationships of AT-SRPs, compared with AT-IRPs.

Earlier studies had just examined the PK profiles of AT from different dosage forms including a floating multiple-unit capsule, a high-density multiple-unit capsule and an IR tablet, showing that the bioavailability of the two gastro retentive preparations with SR characteristics was significantly decreased compared to the IR tablet in male healthy volunteers [12]. However, in the present experiment, there was no statistically significant difference in $AUC_{0-\infty}$ between the two formulations, indicating that they had a similar bioavailability from 0 to infinity in rats. On the contrary, the $AUC_{0-24\,h}$ of the SRPs was significantly lower than that of IRPs, which meant that the bioavailability from 0 to 24 h was significantly different. The results of individual variances confirmed to the expectation that the administration of dosage forms consisting of multiple-units would decrease the inter-subject variability of absorption [12].

However, to extrapolate the results between human and rats, anatomical and physiological features of the GI tract, including surface area, transit time/motility, and enterohepatic circulation, should be considered [25]. Discrepancies in these features among species could affect the absorption sites, as well as the distribution of the absorbed drugs from the oral route [26].

AT, the one of relative β_1-selective blockers, was extensively used to treat cardiovascular diseases. Like other drugs which activate different types of receptors to elicit different pharmacological effects at a wide concentration span, AT has a tendency to lose its selectivity of action at a high plasma concentration and thus causes the adverse effects on respiratory function, peripheral vascular disease and glucose homeostasis through blocking the β_2-receptors [14,18]. Therefore, the minimization of fluctuation in blood concentration for SRPs makes it possible to obtain certain selectivity in pharmacological effect and reduce the potential to cause adverse effects.

The ultimate objective of dosage forms modification is to maximize drug safety and pharmacological response. Compared with IRPs, the fluctuation of drug effects was minimized in SRP despite the E_{max} had delayed. The results conformed to the ideal treatment of hypertension by which the blood pressure was regulated in a certain level. The reduced hypotensive effects fluctuation could be attributed to the change of drug concentrations fluctuation.

$AUEC_{0-\infty}$ values of AT from different formulations were similar, which might be mirrored by equivalence in $AUC_{0-\infty}$. In another hand, $AUEC_{0-24\,h}$ for the two formulations was also similar, but the $AUC_{0-24\,h}$ was significantly different. The results indicating that the drug from SRPs was utilized more completely than IRPS within 24 h. It was interesting to emphasize that these results confirm those previously obtained by Chung et al., who found that despite the $AUC_{0-24\,h}$ for extended-release glipizide was significantly lower than that of immediate-release glipizide, but the two formulations had similar effects on serum concentration of glucose [27]. The results of present study highlight a direct correlation between the magnitude of hypotensive effect (AUEC) and systemic drug exposure (AUC). Currently, researches on this correlation are extremely rare, which always assumed a direct relationship between the plasma drug concentration and effect [14].

Clockwise ECT profiles for SRPs were obtained. It is known that clockwise hysteresis reflects tolerance phenomenon to the

drug induced by desensitization of receptors or production of counter regulatory substances [21]. One study suggested that more pronounced tolerance to the analgesic effects of morphine developed in patients receiving a continuous infusion rather than intermittent intramuscular bolus injections [28]. Similarly, in present work, AT-SRPs was more likely to induce tolerance and this might result from the limited activation of compensatory responses produced by high levels of endogenous agents such as catecholamines following slow input [29]. Therefore, it is necessary to further investigate the tolerance of AT-SRPs at different dosages.

Additionally, the two ECT-curves for SRPs were almost overlapped, suggesting that the presumed effect compartment might be ascribed to the central compartment. Similarly, the estimated PK–PD parameter k_{eo} of AT-SR was significantly greater than that in IR group. This suggests the fast distribution of drug from central compartment to the effect site and the drug could exert hypotensive effect soon after administration.

The counter-clockwise hysteresis loop for AT-IRPs might be caused by disequilibrium between effect site and central compartment. The ECT loop for the effect compartment was leftward to that for the central compartment, suggesting that the AT concentration in effect compartment was lower than that in central compartment at the same effect point. This indicates that there was a distribution course of drug between the two compartments. Pressure-lowering effect of AT-IRPs was fast and short-lasting, which was unfavorable for the treatment of hypertension [30–32].

5. Conclusions

In the present research, the *in vitro* release, pharmacokinetics, pharmacodynamics and PK–PD relationships for AT-SRPs were reported, compared with those for AT-IRPs. The analysis method of AT in plasma was practical. These studies confirmed that the fluctuation of plasma concentration of AT-SRPs in rats was significantly diminished. The effect of AT-SRPs on the treatment of hypertension was maintained in a certain level, which might improve the drug safety. The distribution process of AT between effect-compartment and blood compartment was much faster for SRPs than that for IRPs. Therefore, SRPs would be a desirable delivery vehicle of cardiovascular drugs. In further research, mechanism-based PK–PD models in rats adjusted by parameters concerning anatomical and physiological features of the GI tract need to be established to predict the characteristics of PK and PD in human.

Acknowledgments

This study is financially supported by the major project of National Science and Technology of China for new drugs development (No. 2009ZX09310-004). Thanks Colorcon, ISP, and FMC corporations for providing the excipients, Yong Zhang for the advice on data analysis, and Quanying Bao for the advice on writing.

References

[1] S.R. Vaithiyalingam, S.V. Sastry, R.H. Dehon, I.K. Reddy, M.A. Khan, Long-term stability characterization of a controlled release gastrointestinal therapeutic system coated with a cellulose acetate pseudolatex, Pharmazie 56 (2001) 66–69.
[2] S.V. Sastry, I.K. Reddy, M.A. Khan, Atenolol gastrointestinal therapeutic system: optimization of formulation variables using response surface methodology, J. Control. Release 45 (1997) 121–130.
[3] J.W. Rigby, A.K. Scott, G.M. Hawksworth, J.C. Petrie, A comparison of the pharmacokinetics of atenolol, metoprolol, oxprenolol and propranolol in elderly hypertensive and young healthy subjects, Br, J. Clin. Pharmacol. 20 (1985) 327–331.
[4] J.J. Jiang, L. Tian, Y.L. Huang, Y.S. Li, L. Xu, Pharmacokinetic and pharmacodynamic characteristics of aranidipine sustained-release, enteric-coated tablets in healthy Chinese men: a Phase I, randomized, open-label, single- and multiple-dose study, Clin Ther. 30 (2008) 1290–1299.
[5] S.V. Sastry, M.A. Khan, Aqueous based polymeric dispersion: Plackett–Burman design for screening of formulation variables of atenolol gastrointestinal therapeutic system, Pharm. Acta Helv. 73 (1998) 105–112.
[6] S.V. Sastry, M.A. Khan, Aqueous-based polymeric dispersion: face-centered cubic design for the development of atenolol gastrointestinal therapeutic system, Pharm. Dev. Technol. 3 (1998) 423–432.
[7] P.B. Patil, V.U. Gawali, H.N. Patil, S.R. Hardikar, A.V. Bhosale, Preparation and evaluation of mucoadhesive microspheres of atenolol and propranolol, Int. J. Pharm. Technol. Res. 1 (2009) 639–643.
[8] B. Singh, S.K. Chakkal, N. Ahuja, Formulation and optimization of controlled release mucoadhesive tablets of atenolol using response surface methodology, AAPS PharmSciTech 7 (2006), Article 3 (http://www.aapspharmscitech.org).
[9] J. Kim, S.C. Shin, Controlled release of atenolol from the ethylenevinyl acetate matrix, Int. J. Pharm. 273 (2004) 23–27.
[10] E.R. Kenawy, H.E. Mohamed, S.H. Salem, Controlled release of atenolol from freeze/thawed poly(vinyl alcohol) hydrogel, J. Saudi Chem. Soc. 14 (2010) 237–240.
[11] A. Streubel, J. Siepmann, R. Bodmeier, Floating matrix tablets based on low density foam powder: effects of formulation and processing parameters on drug release, Eur. J. Pharm. Sci. 18 (2003) 37–45.
[12] N. Rouge, E. Allemann, M. Gex-Fabry, L. Balant, E.T. Cole, P. Buri, E. Doelker, Comparative pharmacokinetic study of a floating multiple-unit capsule, a high-density multiple-unit capsule and an immediate-release tablet containing 25 mg atenolol, Pharm. Acta Helv. 73 (1998) 81–87.
[13] L.D. Hu, Y. Liu, X. Tang, Q. Zhang, Preparation and in vitro/in vivo evaluation of sustained-release metformin hydrochloride pellets, Eur. J. Pharm. Biopharm. 64 (2006) 185–192.
[14] A. Hoffman, Pharmacodynamic aspects of sustained release preparations, Adv. Drug. Deliv. Rev. 33 (1998) 185–199.
[15] G. Castaneda-Henandez, G. Caille, P. du Souich, Influence of drug formulation on drug concentration–effect relationships, Clin. Pharmacokinet. 26 (1994) 135–143.
[16] B. Meibohm, H. Derendorf, Pharmacokinetic/pharmacodynamic studies in drug product development, J. Pharm. Sci. 91 (2001) 18–31.
[17] Y.N. Sun, H.J. Lee, R.R. Almon, W.J. Jusko, A pharmacokinetic/pharmacodynamic model for recombinant human growth hormone effects on induction of insulin-like growth factor I in monkeys, J. Pharmacol. Exp. Ther. 289 (1999) 1523–1532.
[18] M.J. Kendall, S.R.J. Maxwell, A. Sandberg, G. Westergren, Controlled release metoprolol: clinical pharmacokinetic and therapeutic implications, Clin. Pharmacokinet. 21 (1991) 319–330.
[19] J. Perez-Urizar, V. Granados-Soto, F.J. Flores-Murrieta, G. Castaneda-Hernandez, Pharmacokinetic–pharmacodynamic modeling: why? Arch. Med. Res. 31 (2000) 539–545.
[20] L.S. Henderson, D.M. Tenero, C.A. Baidoo, A.M. Campanile, A.H. Harter, D. Boyle, T.M. Danoff, Pharmacokinetic and pharmacodynamic comparison of controlled-release carvedilol and immediate-release carvedilol at steady state in patients with hypertension, Am. J. Cardiol. 98 (2006) 17–26.
[21] G.W. Shang, D.N. Liu, L.H. Yan, X.Y. Cui, K.P. Zhang, C. Qi, J. Chen, Nociceptive stimulus modality-related difference in pharmacokinetic–pharmacodynamic modeling of morphine in the rat, Pharmacol. Biochem. Behav. 85 (2006) 464–473.
[22] C.D. Dong, J.P. Liu, W.L. Zhang, P. Liu, L. Chen, Preparation of atenolol sustained-release pellets and its pharmacokinetics in rat, Pharm. Clin. Res. 18 (2010) 231–234.
[23] X.L. Wang, J.L. Feng, Z.X. Wu, M. He, D.G. Li, J.X. Liu, Y.Q. Wu, Y.X. Yu, X.L. Guo, Study on pharmacokinetics of atenolol tablets in old healthy volunteers and nephrotic patients, Chin. Hosp. Pharm. J. 19 (1998) 387–390.
[24] C. Hocht, C. DiVemiero, J.A.W. Opezzo, C.A. Taira, Applicability of microdialysis as a technique for pharmacokinetic–pharmacodynamic (PK–PD) modeling of antihypertensive beta-blockers, J. Pharmacol. Toxicol. 52 (2005) 244–250.
[25] J.M. Desesso, C.F. Jacobson, Anatomical and physiological parameters affecting gastrointestinal absorption in humans and rats, Food Chem. Toxicol. 39 (2001) 209–228.
[26] T.T. Kararli, Comparison of the gastrointestinal anatomy, physiology and biochemistry of humans and commonly used laboratory animals, Biopharm. Drug. Dispos. 16 (1995) 351–380.
[27] M. Chung, I. Kourides, W. Canovatchel, T. Sutfin, M. Messig, R.L. Chaiken, Pharmacokinetics and pharmacodynamics of extended-release glipizide GITS compared with immediate-release glipizide in patients with type II diabetes mellitus, J. Clin. Pharmacol. 42 (2002) 651–657.
[28] H. Marshall, C. Porteous, I. McMillan, S.G. MacPherson, W.S. Nimmo, Relief of pain by infusion of morphine after operation: does tolerance develop? Br. Med. J. Clin. Res. Ed. 291 (1985) 19–21.
[29] D. Murdoch, R.N. Brogden, Sustained release nifedipine formulations: an appraisal of their current uses and prospective roles in the treatment of hypertension, ischaemic heart disease and peripheral vascular disorders, Drugs 41 (1991) 737–776.
[30] C Hocht, C. DiVerniero, J.A. Opezzo, G.F. Bramuglia, C.A. Taira, Pharmacokinetic–pharmacodynamic (PK–PD) modeling of cardiovascular effects of metoprolol in spontaneously hypertensive rats: a microdialysis study, Naunyn Schmiedebergs Arch. Pharmacol. 373 (2006) 310–318.

[31] C. Hocht, C. DiVerniero, J.A.W. Opezzo, C.A. Taira, Pharmacokinetic–pharmacodynamic properties of metoprolol in chronic aortic coarctated rats, Naunyn Schmiedebergs Arch. Pharmacol. 370 (2004) 1–8.

[32] T.J.V. Steeg, J. Freijer, M. Danhof, E.C.M. Lange, Pharmacokinetic–pharmacodynamic modelling of S(−)-atenolol in rats: reduction of isoprenaline-induced tachycardia as a continuous pharmacodynamic endpoint, Br. J. Pharmacol. 151 (2007) 356–366.